

# Distance Relay Element Design

E. O. Schweitzer, III, and Jeff Roberts  
*Schweitzer Engineering Laboratories, Inc.*

Published in the  
SEL *Journal of Reliable Power*, Volume 1, Number 1, July 2010

Previously presented at the  
V Seminário Técnico de Proteção e Controle, August 1995,  
47th Annual Georgia Tech Protective Relaying Conference, April 1993,  
46th Annual Conference for Protective Relay Engineers, April 1993,  
and 1992 ESKOM Protection Conference, November 1992

Previous revised edition released March 1993

Originally presented at the  
19th Annual Western Protective Relay Conference, October 1992

# DISTANCE RELAY ELEMENT DESIGN

Edmund O. Schweitzer, III  
Schweitzer Engineering Labs.  
Pullman, Washington USA

Jeff Roberts  
Schweitzer Engineering Labs.  
Pullman, Washington USA

## INTRODUCTION

All distance relays compare voltages and currents to create impedance-plane and directional characteristics. Electromechanical relays do so by developing torques. Most static-analog implementations use coincidence-timing techniques.

Numerical techniques are the newest way to implement distance and directional relay elements. These relays use torque-like products and other methods to accomplish their operating characteristics. How do these new techniques relate to the classical electro-mechanical and static phase-angle comparators?

This paper presents basic distance and directional element design. A large emphasis is placed on relating the newer digital and numerical methods to the established electromechanical and static-analog methods of designing relay elements.

In addition, we discuss:

- A new method for characterizing distance elements; i.e., equations for mapping points on a relay characteristic onto a single point on a number line.
- How multi-input comparators can be viewed as a family of two-input comparators.
- Which characteristics result from various combinations of comparator inputs.
- Classical element-security problems and remedies.
- A new negative-sequence directional element.
- A different approach to the load-encroachment problem.

Finally, we point out a problem with fault-type selection logic which uses the angle between the negative- and zero-sequence currents. It can select the wrong phase for certain resistive line-line-ground faults. We present a solution to this problem which compares ground and phase fault-resistance estimates.

# PHASE ANGLE COMPARATORS

Phase angle comparators test the angle between various voltage and current combinations to produce directional, reactance, mho, and other characteristics.

This section describes three technologies frequently used to compare phasors in relays: induction cylinders, coincidence timers, and digital multiplication. It also presents a new method: mapping of a characteristic (e.g., a mho circle) onto a point on a number line.

## Induction Cylinder Phase Comparator

Figure 1 is a sketch of an induction cylinder comparator. Assume currents A and B flow in the windings as shown. The cup tends to rotate in the direction of the rotating flux established by the currents. For example, if B leads A, the cup rotates clockwise to close the contacts. If A and B are in phase, the net torque is zero and the cup does not move. This is the only external information available from the relay; either the contacts are open or closed.

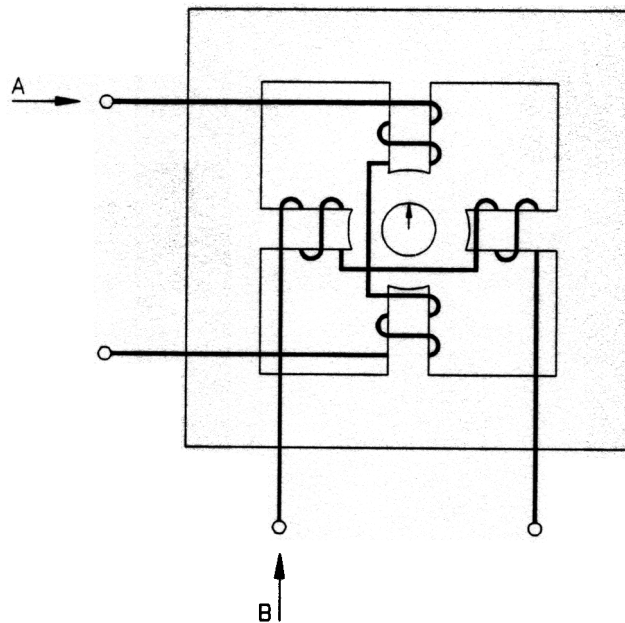


**Figure 1: Induction Cylinder Comparator**

The equation for the cup torque, T, is:

$$T = k \cdot |A| \cdot |B| \cdot \sin \Theta,$$

where  $\Theta$  is the angle between A and B. External circuitry and the coils themselves can be used to modify the torque equation to test other phase relationships.

## Digital Product Phase Comparator

We can easily emulate the behavior of the induction cup element using a computer as part of a digital relay. Given phasors A and B, consider the following complex product:

$$\begin{aligned} S &= A \cdot B^* \\ &= (A_x + j \cdot A_y) \cdot (B_x - j \cdot B_y) \\ &= A_x \cdot B_x + A_y \cdot B_y + j \cdot (A_y \cdot B_x - A_x \cdot B_y) \end{aligned}$$

( \* = complex conjugate)

The angle of the product  $A \cdot B^*$  is the same as the angle of  $A/B$ , and is the angle by which A leads B.

Without loss of generality, assume our phase reference is B, and phasor A leads phasor B by angle  $\Theta$ . In this frame of reference,

$$\begin{aligned} B_x &= |B| & B_y &= 0 \\ A_x &= |A| \cdot \cos \Theta & A_y &= |A| \cdot \sin \Theta \end{aligned}$$

and,

$$S = |A| \cdot |B| \cdot \cos \Theta + j \cdot |A| \cdot |B| \cdot \sin \Theta$$

Separate the real and imaginary parts of  $S = P + j \cdot Q = A \cdot B^*$ :

$$\begin{aligned} P &= |A| \cdot |B| \cdot \cos \Theta \\ Q &= |A| \cdot |B| \cdot \sin \Theta \end{aligned}$$

Both P and Q are two-input phase angle comparators. The P-comparator has a maximum "torque" when A and B are in phase. The Q-comparator has maximum torque when the two inputs are in quadrature. The Q-comparator is essentially the same as the induction cylinder with current inputs.

In digital relays, is it easy to save the torques (P, Q). We can use the sign of the result (analogous to the cup rotation direction) as well as the magnitudes for tests involving fault type, sensitivity, etc.

## Coincidence-Timing Two-Input Phase Comparator

To test the phase angle between sinusoids a and b, we can first convert a and b to square waves to derive signals A and B. The time coincidence of A and B is shown in Figure 2.

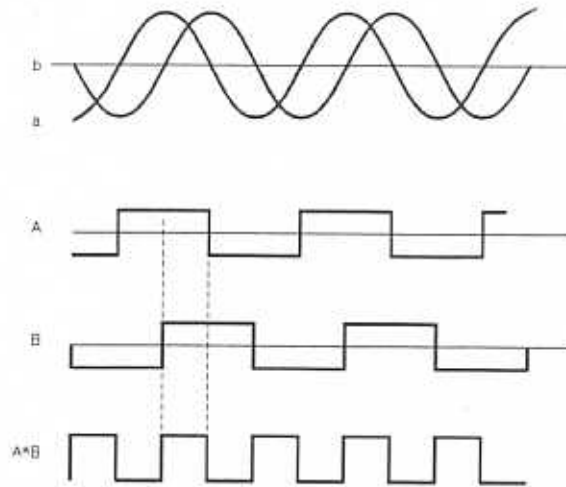
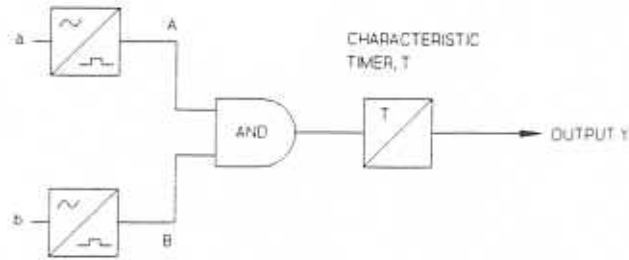


**Figure 2: Coincidence-Timing Two-Input Comparator Logic**

One advantage of this comparator is the characteristic timer setting  $T$  controls the phase angle of coincidence required to obtain an output  $y$ , so we can easily synthesize mho, lenticular, and tomato characteristics.

### Application of Digital Product Phase Comparator

A mho element tests the angle between a line-drop-compensated voltage and a polarizing or reference voltage.

- Let  $\delta V = (r \cdot Z \cdot I - V)$ , where  $\delta V$  is the line-drop compensated voltage  
 $Z$  = replica line impedance  
 $r$  = per-unit reach in terms of the replica impedance  
 $I$  = measured current  
 $V$  = measured voltage  
 $V_p$  = polarizing voltage.

We need to test the angle between  $\delta V$  and  $V_p$ . When the angle is  $90^\circ$ , the relationship between  $\delta V$  and  $V_p$  is any point on the circle, as shown in Figure 3.

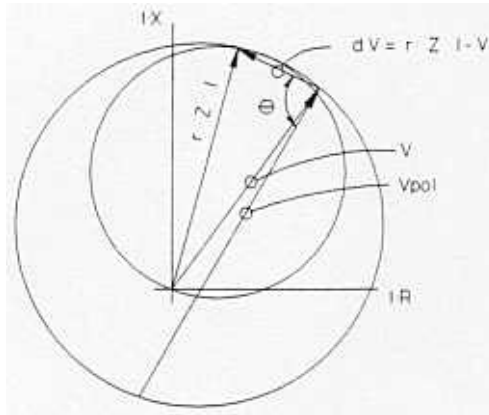


**Figure 3: Mho Element Derivation**

Let us test  $\delta V$  and  $V_p$  using a digital product comparator. Which one should we use -- sine or cosine? Since balance (or zero torque) is at  $90^\circ$ , we need to use the cosine comparator, because  $\cos 90^\circ = 0$ .

$$\text{Let } P = \text{Re}[\delta V \cdot V_p^*]$$

Then:  $P > 0$  represents the area inside the circle of reach  $r \cdot Z$   
 $P = 0$  represents the circle itself  
 $P < 0$  represents the area outside the circle of reach  $r \cdot Z$

(Re = real portion)

### Characteristic-Mapping Approach

Traditionally, one comparator is required for each zone, and for each voltage and current input combination. We can achieve significant economy in processing with no loss in performance by mapping the points on any mho circle of reach  $r$  onto a unique point on a number line.

Recall the mho comparator, P:

$$\begin{aligned} P &= \text{Re}[\delta V \cdot V_p^*] \\ &= \text{Re}[(r \cdot Z \cdot I - V) \cdot V_p^*] \end{aligned}$$

For any  $V, I, V_p$  combination on a circle of reach  $r$ , P is zero. This condition of balance is:

$$0 = \text{Re}[(r \cdot Z \cdot I - V) \cdot V_p^*]$$

Solving for  $r$  yields in an equation which is the reach of the mho circle corresponding to the condition of balance:

$$r = \frac{\text{Re}(V \cdot V_p^*)}{\text{Re}[Z \cdot I \cdot V_p^*]} \quad \text{Equation 1}$$

**Observations:**

- 1 Equation 1 maps all the points on any mho circle of reach  $r$  onto a single point on the number line. If we need four mho circles, we no longer require four comparators. Instead, we simply need four tests of the calculated  $r$ .

For example, a Zone 1 mho circle test might test  $r$  against 0.85, which represents a reach of 85%. Figure 4 illustrates mapping of mho circles into points for a four zone relay.

2. Because  $V$  could be zero, we cannot rely on the sign of  $r$  to reliably indicate direction. Fortunately, the denominator of the  $r$ -equation is a directional element because it tests the angle between a voltage and a current. The sign of the denominator reliably indicates fault direction.

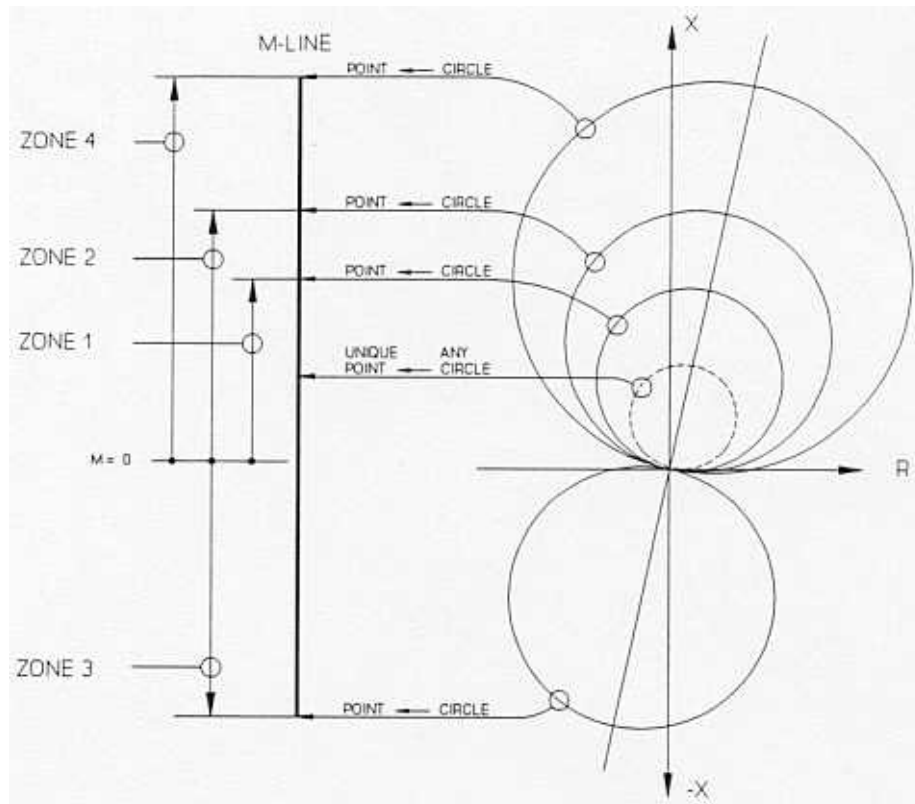


**Figure 4: Each Mho Circle Maps onto a Point on the M-Line**

**MULTIPLE-INPUT COMPARATORS ARE REALLY A FAMILY OF TWO-INPUT COMPARATORS**

Multi-input comparators are widely used in distance relays. These comparators can be easily understood by representing them as several two-input comparators.

The top of Figure 5 shows a three-input comparator. If inputs X, Y, and Z overlap by at least 90°, then output T asserts.

What characteristic does a multiple-input comparator provide?

The answer is simply the intersection of three two-input comparator characteristics, using pairs (X,Y), (Y,Z), and (Z,X). This arrangement is shown in the bottom of Figure 5.

Refer to the coincidence timing diagram shown in the middle of Figure 5. Assume signals X and Y are slightly less than  $90^\circ$  apart, so we barely produce an output if X and Y were the only two inputs. Input Z does not interfere with the output as long as its leading edge is between the leading edges of X and Y. (Assuming all pulses are  $180^\circ$  wide, we need not make the parallel argument about the trailing edges.)

The first condition is X and Y overlap by at least  $90^\circ$ . The two-input comparator XY represents this condition. The second condition is that the leading edge of Z lies between the leading edges of X and Y. The ZX conditions ensures that Z is within  $\pm 90^\circ$  of X. The YZ condition ensures that Z is within  $\pm 90^\circ$  of Y.

If Z leads X, then we lose the YZ output. If Z lags Y then we lose the ZX output. Therefore Z must be between X and Y, which is the same condition we noted for the three-input comparator.

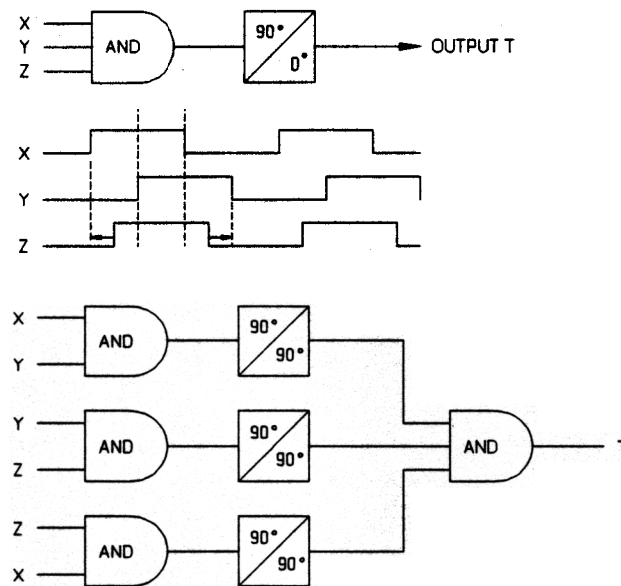


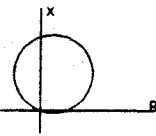
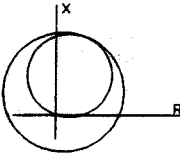
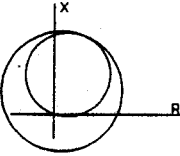
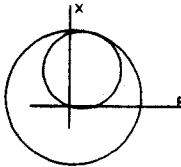
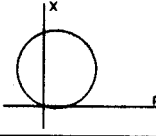
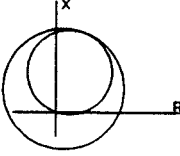
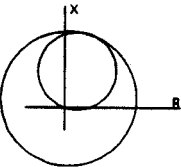
Figure 5: Coincidence-Timing Multi-Input Logic

## A QUICK REVIEW OF MHO ELEMENT POLARIZING CHOICES

Mho elements compare the angle between  $(Z \cdot I - V)$  and  $V_p$ . There are many choices for the polarizing voltage,  $V_p$ . Table 1 reviews some of them.



**Table 1: Mho Element Polarizing Choices**

Operating	Polarizing	Characteristic	General Comments
$(Z \cdot I_{bc} - V_{bc})$	$V_{bc}$ (self pol.)		<ul style="list-style-type: none"> <li>• No expansion.</li> <li>• Unreliable for zero-voltage faults.</li> <li>• Directionally insecure for reverse bus faults during high load. Requires additional directional element.</li> </ul>
$(Z \cdot I_{bc} - V_{bc})$	$-j \cdot V_a$ (cross pol. w/o memory)		<ul style="list-style-type: none"> <li>• Good expansion for <math>\phi</math>-<math>\phi</math> faults.</li> <li>• Unreliable for zero-voltage 3<math>\phi</math> faults.</li> <li>• Reverse bus fault security problems during high load periods. Requires additional directional element.</li> </ul>
$(Z \cdot I_{bc} - V_{bc})$	$-j \cdot V_{a,mem}$ (cross pol. w/ memory)		<ul style="list-style-type: none"> <li>• Good expansion for phase faults.</li> <li>• Reliable operation for zero-voltage 3<math>\phi</math> faults until pol. memory expires.</li> <li>• Rev. <math>\phi</math>-<math>\phi</math> bus fault security problems during high load periods. Requires additional directional element.</li> <li>• Single-pole trip applications require study for pole-open security.</li> </ul>
$(Z \cdot I_{bc} - V_{bc})$	$-j \cdot V_{a,mem}$ (pos.-seq. mem. pol.)		<ul style="list-style-type: none"> <li>• Greatest characteristic expansion for <math>\phi</math>-<math>\phi</math> and 3<math>\phi</math> faults.</li> <li>• Reliable operation for zero-voltage 3<math>\phi</math> faults until pol. memory expires.</li> <li>• Rev. <math>\phi</math>-<math>\phi</math> bus fault security problems during high load periods. Requires additional directional element.</li> <li>• Best single-pole trip security.</li> </ul>
$[Z \cdot (I) - V_a]$  $I = I_a + k \cdot I_r$	$V_a$ (self pol.)		<ul style="list-style-type: none"> <li>• No expansion.</li> <li>• Unreliable for zero voltage single-line-ground faults.</li> <li>• Requires directional element.</li> </ul>
$[Z \cdot (I) - V_a]$  $I = I_a + k \cdot I_r$	$j \cdot V_{bc}$ (cross pol.)		<ul style="list-style-type: none"> <li>• Good expansion.</li> <li>• Reliable operation reliable for zero-voltage single-line-ground faults.</li> <li>• Requires directional element.</li> <li>• Single-pole trip applications require study for pole-open security.</li> </ul>
$[Z \cdot (I) - V_a]$  $I = I_a + k \cdot I_r$	$V_{a,mem}$ (pos.-seq. mem. pol.)		<ul style="list-style-type: none"> <li>• Greatest expansion.</li> <li>• Reliable operation for zero voltage ground faults.</li> <li>• Requires directional element.</li> <li>• Best single-pole trip security.</li> </ul>

The positive-sequence memory-polarized elements are generally preferred. The benefits include:

- The greatest amount of expansion for improved resistive coverage. These elements always expand back to the source.
- Memory action for all fault types. This is very important for close-in 3 $\phi$  faults.
- A common polarizing reference for all six distance-measuring loops. This is important for single-pole tripping, during a pole-open period.

## CREATING QUADRILATERAL GROUND DISTANCE CHARACTERISTICS

The quadrilateral characteristic requires four tests:

- Reactance test (top line)
- Positive and negative resistance tests (sides)
- Directional test (bottom)

### Ground Distance Reactance Comparator

A reactance element tests the angle between the line-drop-compensated voltage and the polarizing current.

- Let  $\delta V = (r \cdot Z \cdot I - V)$ , where  $\delta V$  is the line-drop compensated voltage  
 $Z1 =$  replica positive-sequence line impedance  
 $Z0 =$  replica zero-sequence line impedance  
 $r =$  per-unit reach in terms of the replica impedance  
 $I =$  phase current plus the residual current compensated by  $k = (Z0 - Z1)/3 \cdot Z1$   
 $V =$  measured voltage  
 $I_p =$  polarizing current.

We need to test the angle between  $\delta V$  and  $I_p^*$ . When the angle is  $0^\circ$ , the impedance is on the line shown in Figure 6.

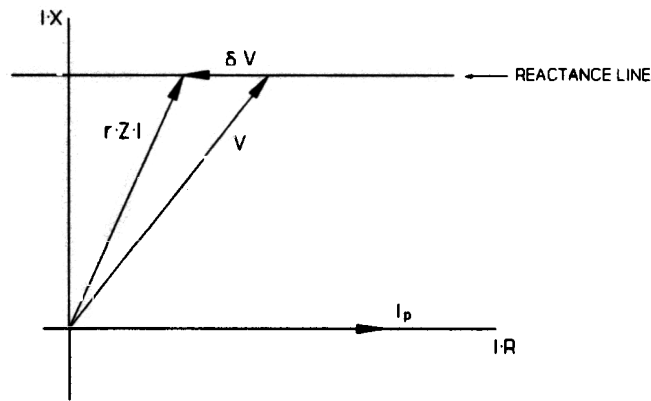


**Figure 6: Ground Distance Reactance Element Derivation**

Again, using a digital product comparator, test the angle between  $\delta V$  and  $I_p$ . The correct comparator to use is the sine comparator, since the balance point is  $0^\circ$ .

Let  $Q = \text{Im}[\delta V \cdot I_p^*]$ ; (Im = imaginary portion)

Then:  $Q < 0$  represents the area above the line with reach  $r \cdot X$   
 $Q = 0$  represents the line itself  
 $Q > 0$  represents the area below the line of reach  $r \cdot X$

This element must measure line reactance without adverse affects from fault resistance or load flow. Phase currents are poor choices for the polarizing reference, because they make the reactance element severely under- or overreach, depending on the flow of load current. Negative-sequence or residual currents are appropriate polarizing choices.

In some non-homogeneous system applications, the tip produced by  $I_p$  may be insufficient to prevent overreach. To compensate, we can introduce an angle bias, or tip, to the reactance characteristic, or else reduce the reach of the Zone 1 element.

### Ground Fault Directional Element

Directional elements for ground fault must operate at fault current levels well-below the magnitude of load currents. Negative- and zero-sequence currents and voltages are mainly due to faults, and therefore are good choices for directional elements.

System unbalance and measurement errors ultimately limit the sensitivity of directional elements based on negative- or zero-sequence components.

Let  $V_{\text{seq}}$  = measured sequence voltage ( $V_2$  or  $V_0$ )  
 $I_{\text{seq}}$  = measured sequence current ( $I_2$  or  $I_0$ )  
 $Z$  = impedance whose angle adjusts  $I_{\text{seq}}$

When the angle between  $-V_{\text{seq}}$  and  $Z \cdot I_{\text{seq}}$  is  $0^\circ$ , the directional comparator has maximum torque. A basic negative-sequence implementation of this concept is shown in Figure 7.

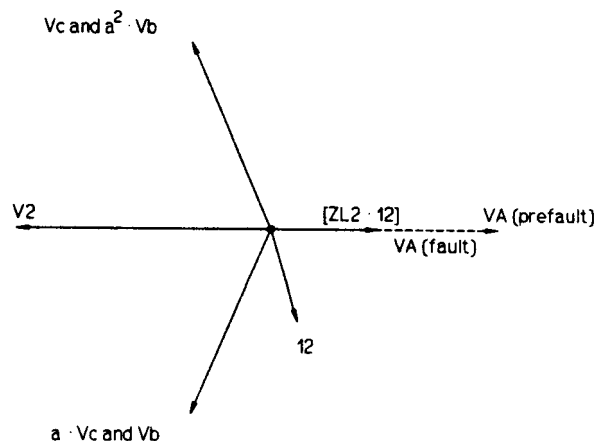


**Figure 7: Negative-Sequence Directional Element**

The cosine comparator gives a maximum output when the angle between the two inputs is zero degrees.

$$\text{Let } P = \text{Re}[V_{\text{seq}} \cdot (Z \cdot I_{\text{seq}})^*];$$

Then:  $P < 0$  represents the area above the zero-torque line (forward)

$P = 0$  represents the zero torque line

$P > 0$  represents the area below the zero-torque line (reverse)

### Resistance Tests

Rather than using two separate comparators, we shall apply the digital-mapping method to calculate the apparent resistance and test it against left and right side resistance thresholds.

For an  $A\phi$ -ground fault on the system in Figure 8, the  $A\phi$ -ground voltage at Bus S is:

$$V_A = m \cdot Z_{1L} \cdot (I_{AS} + k_0 \cdot I_{RS}) + R_{AF} \cdot I_F \quad \text{Equation 2}$$

Where:

- $V_A$  =  $A\phi$  voltage measured at Bus S
- $m$  = per-unit distance to the fault from Bus S
- $R_{AF}$  =  $A\phi$  fault resistance
- $I_F$  = total current flowing through  $R_F$
- $I_{AS}$  =  $A\phi$  current measured at Bus S
- $I_{RS}$  = residual current measured at Bus S ( $3I_{0S}$ )

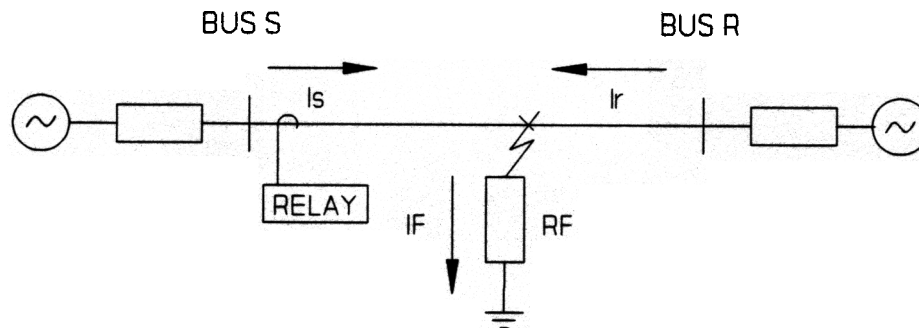


**Figure 8: System One Line Diagram with SLG Fault**

The goal is to extract  $R_{AF}$  from Equation 2. We must eliminate the line-drop voltage term,  $m \cdot Z_{1L} \cdot (I_{AS} + k_0 \cdot I_{RS})$ , save the imaginary components, and solve for  $R_{AF}$ . The result is:

$$R_{AF} = \frac{\text{Im}[V_A \cdot (Z_{1L} \cdot (I_{AS} + k_0 \cdot I_{RS}))^*]}{\text{Im}[I_F \cdot (Z_{1L} \cdot (I_{AS} + k_0 \cdot I_{RS}))^*]}$$

The denominator contains  $I_F$ , which includes fault and load current from both ends of the line.

However, only Bus S currents are available to the relay at Bus S. We need to approximate  $I_F$  in terms of Bus S current components. The approximation must be minimally system and load dependent. This last requirement permits setting the resistive thresholds with less concern that the resistive boundaries might be crossed under balanced load-flow conditions.

Let  $I_F = 3/2 \cdot (I_{2S} + I_{0S})$ , where  $I_{2S}$  and  $I_{0S}$  are the Bus S negative- and zero-sequence currents respectively. This current combination has all the available fault information, except the positive-sequence current ( $I_1$ ). We specifically ignore  $I_1$  because it is heavily influenced by load flow.

Then:

$$R_{AF} = \frac{\text{Im}[V_A \cdot (Z_{1L} \cdot (I_{AS} + k_0 \cdot I_{RS}))^*]}{\text{Im}[3/2 \cdot (I_{2S} + I_{0S}) \cdot (Z_{1L} \cdot (I_{AS} + k_0 \cdot I_{RS}))^*]} \quad \text{Equation 3}$$

With this substitution, the fault resistance estimate of Equation 3 is independent of balanced load. The 3/2 scale factor accounts for the missing  $I_1$  contribution and ensures  $R_{AF}$  measures the true fault resistance on a radial system. Infeed from Bus R causes  $R_{AF}$  to increase, because our substitution for  $I_F$  does not include any measurement of current from Bus R. For example, if the impedances on either side of the fault are equal,  $R_{AF}$  is half the actual fault resistance.

This method provides an easy means of testing  $R_{AF}$  for both the left and right sides of the quadrilateral element: calculate R and test the result against  $\pm R$  thresholds for each zone.

For example, a Zone 1 resistive boundary might test  $R_{AF}$  against  $\pm 2\Omega$ . If the result is  $1\Omega$ , this satisfies the criteria set for the Zone 1 quadrilateral resistive checks.

## MAINTAINING DIRECTIONAL SECURITY

Directional security is paramount. At first glance, mho elements appear directional. However, some safeguards are required to ensure security.

### Ground Direction Security Concerns

**Reverse Ground Faults:** The operating quantities for all ground distance elements include residual current. For example, the residual current produced by a reverse  $A\phi$  ground fault is also used in the phase-ground distance elements for B and C phases. The residual current can cause a forward-reaching  $B\phi$  or  $C\phi$  ground distance element to operate. We can avoid this problem by supervising the ground distance elements with a directional element, by a phase-selection comparator, or by introducing additional conditions in a multiple-input comparator.

## Selection of Directional Element Input Quantities

Negative-sequence directional elements have notable advantages:

- Insensitivity to zero-sequence mutual coupling.
- There is generally more negative-sequence current than zero-sequence current for remote ground faults with high fault resistance. This allows higher sensitivity with reasonable and secure sensitivity thresholds.
- Insensitivity to vt neutral shift, possibly caused by multiple grounds on the vt neutral.

Perhaps the major disadvantage is negative-sequence elements are rendered useless when one or two poles of the breaker are open.

## Compensated Negative-Sequence Directional Element

When the negative-sequence source behind the relay terminal is very strong, the negative-sequence voltage ( $V_2$ ) at the relay can be very low, especially for remote faults.

To overcome low  $V_2$  magnitude, we can add a compensating quantity which boosts  $V_2$  by  $(\alpha \cdot Z_{L2} \cdot I_2)$ . The constant  $\alpha$  controls the amount of compensation.

Equation 4 shows the torque equation for a compensated negative-sequence directional element.

$$T_{32Q} = \text{Re}[(V_2 - \alpha \cdot Z_{L2} \cdot I_2) \cdot (Z_{L2} \cdot I_2)^*] \quad \text{Equation 4}$$

The term  $(\alpha \cdot Z_{L2} \cdot I_2)$  adds with  $V_2$  for forward faults, and subtracts for reverse faults. Setting  $\alpha$  too large can make a reverse fault appear forward. This results when  $(\alpha \cdot Z_{L2} \cdot I_2)$  is greater but opposed to the measured  $V_2$  for reverse faults.

## Relationship of the Apparent $Z_2$ to Fault Direction

The sequence network for a ground fault at the relay bus is shown in Figure 9. The relay measures  $IS_2$  for forward faults, and  $-IR_2$  for reverse faults.

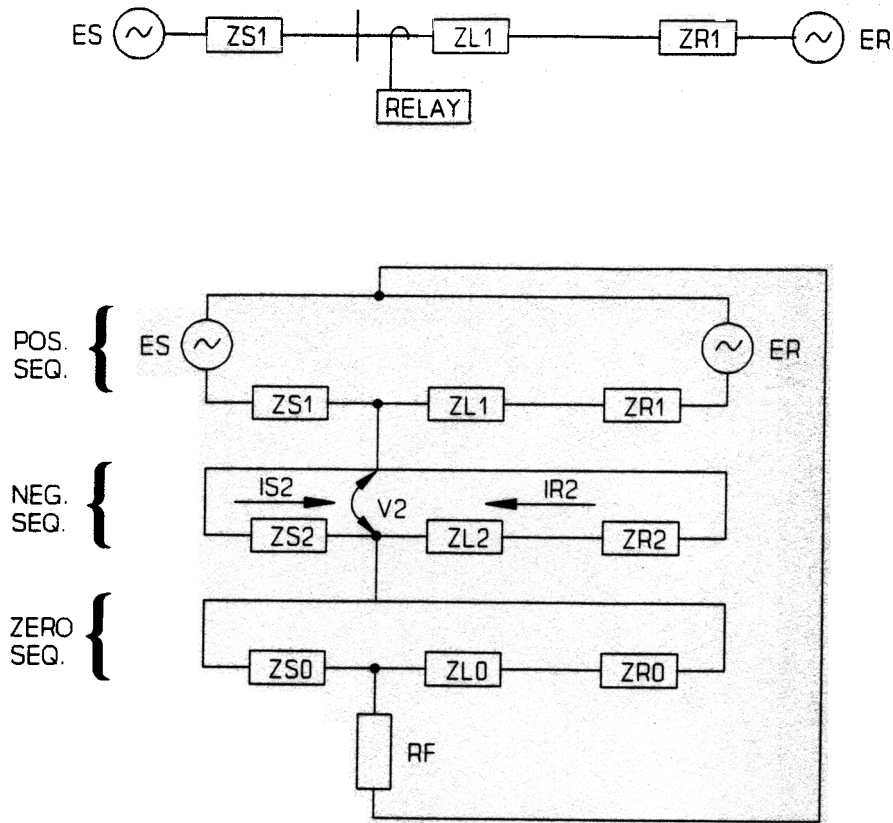


**Figure 9: Sequence Network for a Reverse Single-Line-Ground Fault**

From  $V_2$  and  $I_2$ , calculate  $Z_2$ :

$$\text{Forward SLG Faults: } Z_2 = \frac{-V_2}{I_2} = -Z_{S2}$$

$$\text{Reverse SLG Faults: } Z_2 = \frac{-V_2}{-I_2} = (Z_{L2} + Z_{R2})$$

This relationship is shown in Figure 10 for a  $90^\circ$  system.

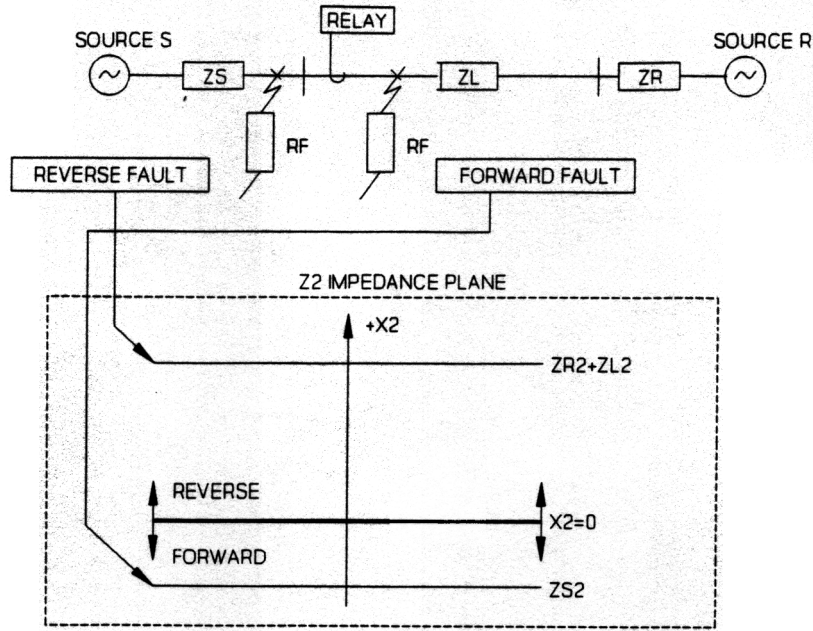


**Figure 10: Measured Negative-Sequence Impedance Yields Direction**

For the system in Figure 10, the fault is forward if  $Z2$  is negative, and reverse if  $Z2$  is positive.

### Negative-Sequence Directional Element Based on Calculating and Testing $Z2$

The discussion above shows that calculated  $Z2$  could be used to determine fault direction.

Recall the compensated negative-sequence directional element equation, T32Q:

$$T32Q = \text{Re}[(V2 - \alpha \cdot ZL2 \cdot I2) \cdot (ZL2 \cdot I2)^*]$$

The forward/reverse balance condition for this element is zero torque. This is:

$$0 = \text{Re}[(V2 - \alpha \cdot ZL2 \cdot I2) \cdot (ZL2 \cdot I2)^*]$$

$$\begin{aligned} \text{Let } \alpha &= z2 \\ ZL2 &= 1 \angle \theta \text{ where } \theta \text{ is the angle of } ZL2 \end{aligned}$$

Substituting,

$$0 = \text{Re}[(V2 - z2 \angle \theta \cdot I2) \cdot (I2 \cdot 1 \angle \theta)^*]$$



Solving for  $z_2$  results in an equation corresponding to the condition of zero-torque:

$$z_2 = \frac{\text{Re}[V_2 \cdot (I_2 \cdot 1 \angle \Theta)^*]}{\text{Re}[(I_2 \cdot 1 \angle \Theta) \cdot (I_2 \cdot 1 \angle \Theta)^*]}$$

$$z_2 = \frac{\text{Re}[V_2 \cdot (I_2 \cdot 1 \angle \Theta)^*]}{|I_2|^2}$$

Recall the  $(\alpha \cdot Z_{L2} \cdot I_2)$  term increases the amount of  $V_2$  for directional calculations. This is equivalent to increasing the magnitude of the negative-sequence source behind the relay location. This same task is accomplished by increasing the forward  $z_2$  threshold.

The criteria for declaring forward and reverse faults are then:

- If  $z_2 < \text{forward threshold}$ , then the fault is forward  
 $z_2 > \text{reverse threshold}$ , then the fault is reverse

The forward threshold must be less than the reverse threshold to avoid any overlap.

The  $z_2$  directional element has all of the benefits of both the traditional and compensated negative-sequence directional element. It also provides better visualization of how much compensation is secure and required. Set the forward and reverse impedance thresholds based upon the strongest source conditions.

### Phase-Phase Distance Element Security for Reverse Phase-Phase Faults

Phase-phase distance elements use phase-phase currents. For example, a BC phase-phase distance element uses  $I_{BC}$  or  $(I_B - I_C)$ . For a close-in reverse CA fault, the  $C\phi$  current can cause operation of the forward-reaching BC element. An easy way to avoid this risk is by supervising the phase-phase distance elements with the negative-sequence direction element just described. (The negative-sequence directional element is ignored for  $3\phi$  faults which pick up all three phase-phase distance elements.)

### Phase-Phase Distance Element Security for Reverse Three-Phase Faults

Phase distance elements require memory polarization to be secure and reliable for reverse three-phase ( $3\phi$ ) faults.

The most onerous  $3\phi$  fault is one with the following qualifications:

1. A small critical amount of fault resistance.
2. Significant load flow into the bus from a weaker source.

Three-phase faults are a concern to phase distance elements only after the memory expires. For bolted faults, each phase voltage is zero. Once the memory expires, the distance elements are disabled. However, with some resistance, the polarization voltage does not go to zero, and could move to an angle permitting tripping.

Figure 11.a illustrates a system with a reverse 3 $\phi$  fault with fault resistance. Figure 11.b shows the total A $\phi$  fault current ( $I_{F,a}$ ), the prefault memory voltage ( $V_{a,mem}$ ), A $\phi$  voltage and current seen by the relay ( $V_{af}$  and  $I_{RLY,a}$  respectively), and  $I_{RLY,a}$  adjusted by the replica line impedance.

Recall the denominator term of Equation 1 for a phase distance element. This denominator term is a directional element. It indicates how a phase distance element of infinite reach would perform for this same fault. If the angle between  $Z \cdot I$  and  $V_p$  is less than  $90^\circ$ , the phase distance element declares the fault forward. From Figure 11.b, the angle between  $I_{RLY,a} \cdot Z$  and  $V_a$  is less than  $90^\circ$ . Thus, after the memory voltage ( $V_{a,mem}$ ) becomes in step with  $V_{af}$ , the directional security of the phase distance element is compromised.

Figure 11.c illustrates the same reverse 3 $\phi$  fault with load flowing out from the relay terminal (from  $E_s$  towards  $E_R$ ). For this case, the phase distance relay is secure even after the memory voltage becomes in-step with the fault voltage.

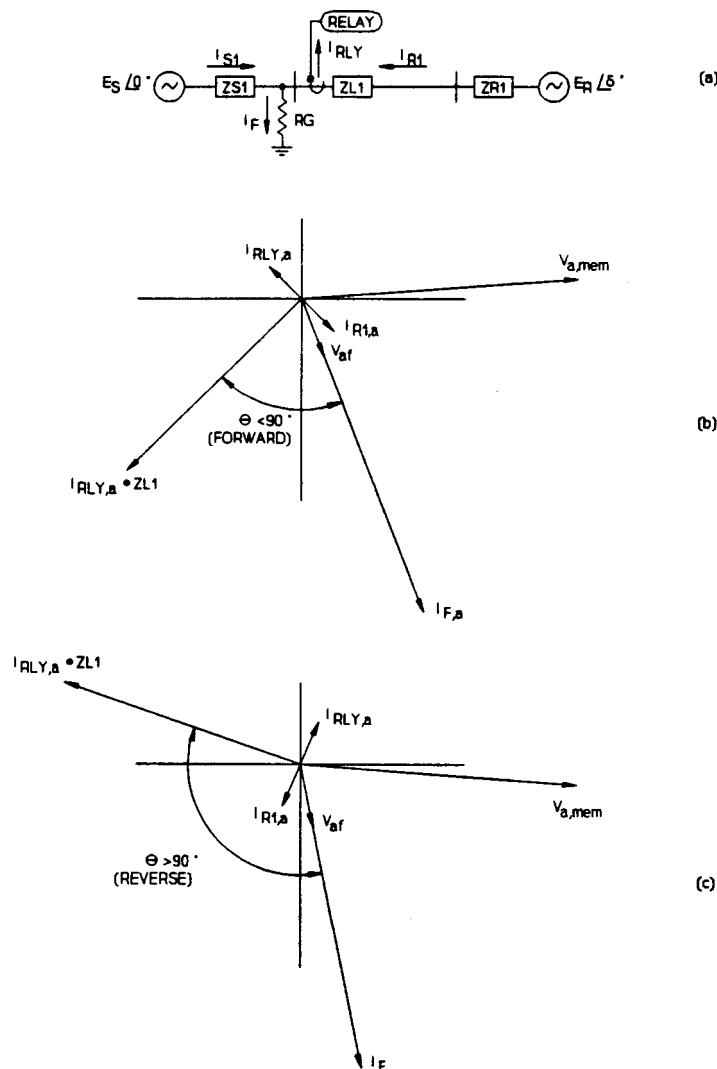


Figure 11: Reverse 3 $\phi$  Fault Conditions and Mho Element Performance

## Solutions

1. Clear the  $3\phi$  fault before the memory expires.
2. The apparent impedance for the reverse  $3\phi$ -G fault enters the tripping characteristic in the second-quadrant. Reducing the maximum torque angle reduces the amount of second-quadrant coverage.
3. Require an increased torque magnitude output from the comparator (i.e., desensitize the element). As the apparent impedance enters the tripping characteristic very near the origin, forward direction  $3\phi$  faults produce greater torques than do the reverse  $3\phi$  faults.
4. Add current offset in the positive direction to the polarizing reference.
5. Test the angle between the positive-sequence current and voltage (i.e., use a positive-sequence directional element). This angular test limits the three-phase fault coverage to a  $180^\circ$  impedance angle sector of  $-120^\circ$  to  $60^\circ$ .

## LOAD ENCROACHMENT

The impedance of heavy loads can actually be less than the impedance of some faults. Yet, the protection must be made selective enough to discriminate between load and fault conditions. Unbalance aids selectivity for all faults except three-phase faults.

Figure 12 shows the load-encroachment characteristics in the impedance plane.

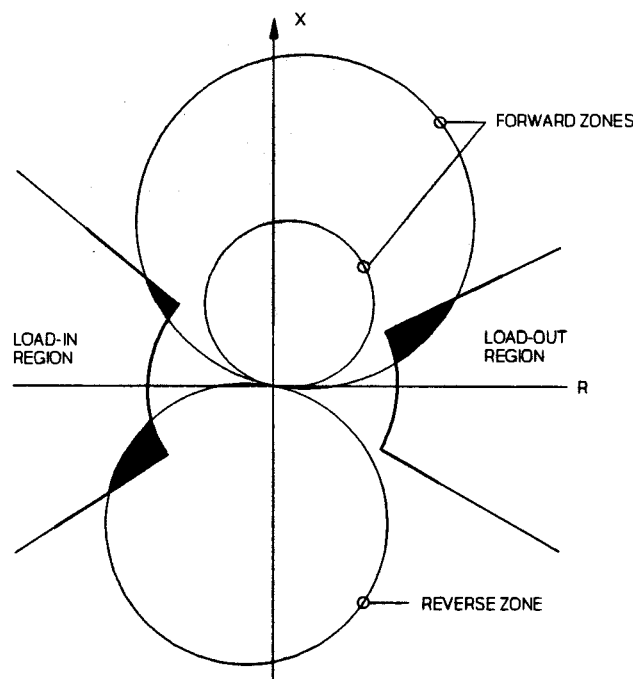


**Figure 12: Load Encroachment on Mho Distance Element Characteristics**

When power flows out, the load impedance is in the wedge-shaped load-impedance area to the right of the X-axis. When power flows in, the load impedance is in the left-hand load-impedance area.

There is overlap (shaded solid) between the mho circle and the load areas. Should the load impedance lie in the shaded area, the impedance relay will detect the under-impedance condition and trip the heavily-loaded line. Such protection unnecessarily limits the load-carrying capability of the line.

For better load rejection, the mho circle can be squeezed into a lenticular or elliptical shape. Unfortunately, this also reduces the fault coverage.

Alternatively, we could use additional comparators to make blinders parallel to the transmission line characteristic, to limit the impedance-plane coverage, and exclude load from the tripping characteristic.

Or, we could build quadrilateral characteristics, which box-out load.

All traditional solutions have the same common approach: shape the operating characteristic of the relay to avoid load. The traditional solutions have two major disadvantages:

1. Reducing the size of the relay characteristic desensitizes the relay to faults with resistance. Avoiding a small area of load encroachment often requires sacrificing much larger areas of fault coverage.
2. From a user's point of view, the more complex shapes become hard to define, and the relays are harder to set.

A new approach does not modify the relay characteristic shape directly. Instead, it defines the load regions in the impedance plane, and blocks operation of distance elements if the impedance is in either of the load regions.

Figure 13 shows the new approach applied to a four-zone mho relay. The mho characteristics are conventional, and are not modified to exclude load.

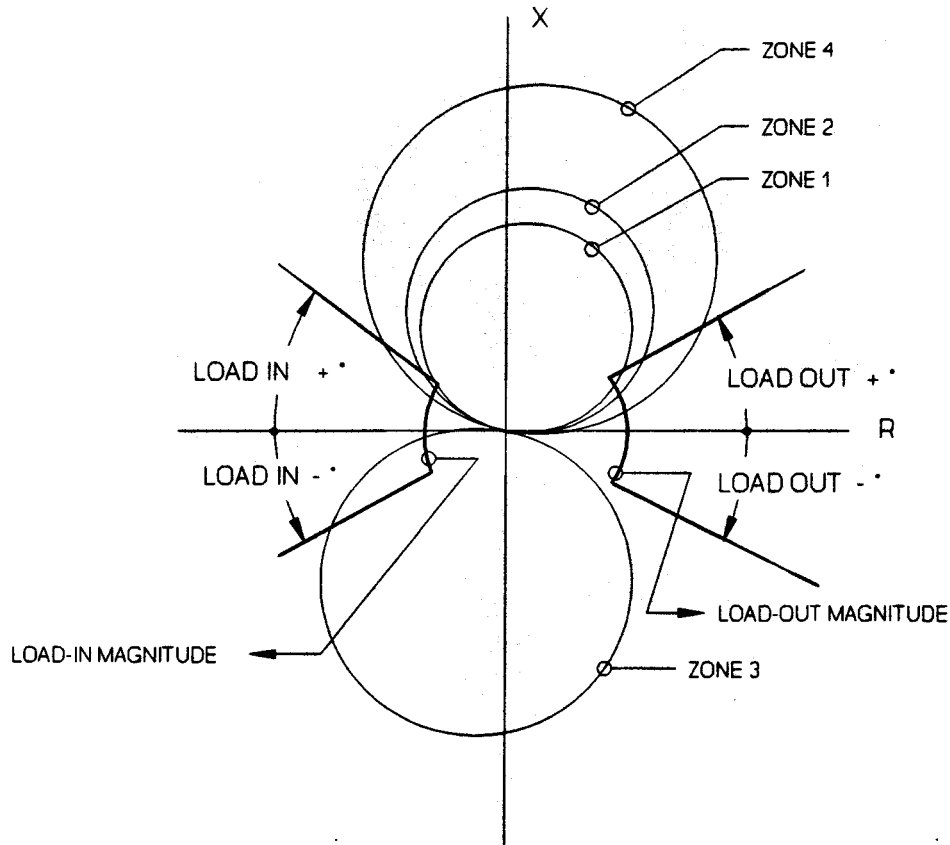


**Figure 13: Improved Load-Encroachment Method**

There are two load regions shown (load-in and load-out). The relay calculates the complex positive-sequence impedance and tests it against the boundaries of these load regions. If the impedance is inside either region, then the relay concludes the impedance represents load, and blocks the mho elements. If the impedance is outside both load regions, the mho elements are permitted to operate.

The advantages of the new approach include:

1. Greater coverage for faults is possible because only the overlap between the load characteristic and the relay characteristic is blocked.
2. The load-encroachment characteristics are easy to set, because they can be directly related to the maximum load conditions. Once we have maximum load-in and load-out conditions, and the range of power factors of the load, the load-impedance areas can be found. No customization of relay characteristics is required to avoid load.
3. Separate characteristics for load-in and load-out are easy to define.
4. Since the characteristics for faults and loads are independent, there is less chance of setting errors.

The logic applies to three-phase faults only. Load-encroachment blocking is not required or desired for unbalanced faults (e.g., AB, BC, CA, AG, BG, CG, ABG, BCG, CAG faults).

## FAULT-TYPE SELECTION CONSIDERATIONS

For security, distance relay schemes must consider the behavior of the distance elements in all six fault loops (AG, BG, CG, AB, BC, and CA) under very broad and general system, load, and fault conditions.

There are two major concerns:

- Ground distance elements can overreach for line-line-ground (LLG) faults.
- Phase distance elements can operate for close-in line-ground (LG) faults.

The first concern is generally considered a problem in all applications. The second concern is a problem in single-pole-trip schemes, and a targeting nuisance.

How can we reliably prevent unwanted relay elements from interfering with the performance of the overall scheme?

If we know the fault is an AG fault, then we can block the AB and CA elements in order to avoid a three-pole trip for a LG fault.

If we know the fault is a BCG fault, then we can block the BG and CG elements, avoiding possible overreach by the BG and CG elements.

(The BG element tends to overreach for a BCG fault with resistance to ground. The CG element tends to overreach for a BCG fault with resistance between the phases.)

### Selection Using the Angle Between $I_0$ and $I_2$

The angle between the negative-sequence current and the zero-sequence current is a frequently used and very useful indicator.

Figure 14 shows the sequence networks for AG and BCG faults. The symmetrical component currents are referenced to phase A. That is,  $I_0$  means  $I_{A0}$ , and  $I_2$  means  $I_{A2}$ . For these two faults, the angle between  $I_2$  and  $I_0$  is zero degrees. Figure 15 shows phasor diagrams for AG, BG, and CG faults. It also shows the phase relationships between  $I_0$  and  $I_2$  for the three faults.

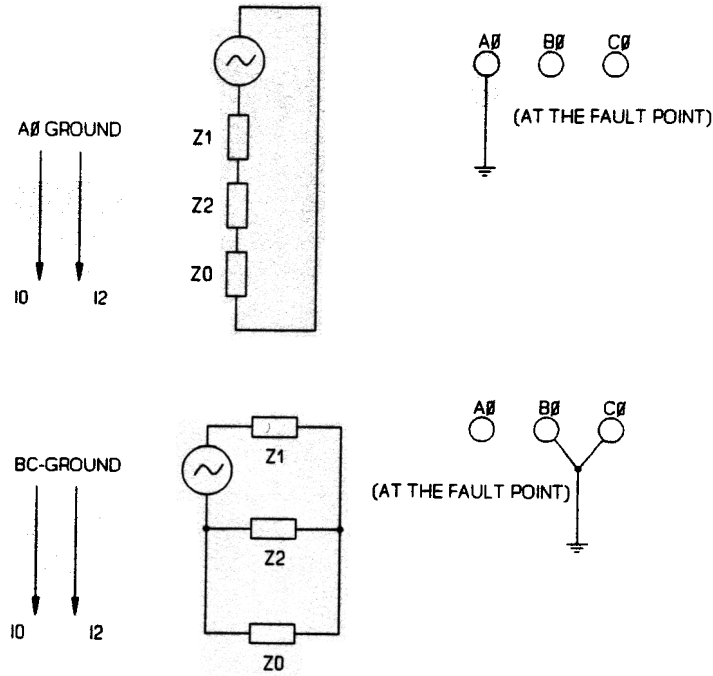


**Figure 14:  $I_0$  and  $I_2$  Relationship for AG and BCG Faults (without Fault Resistance)**

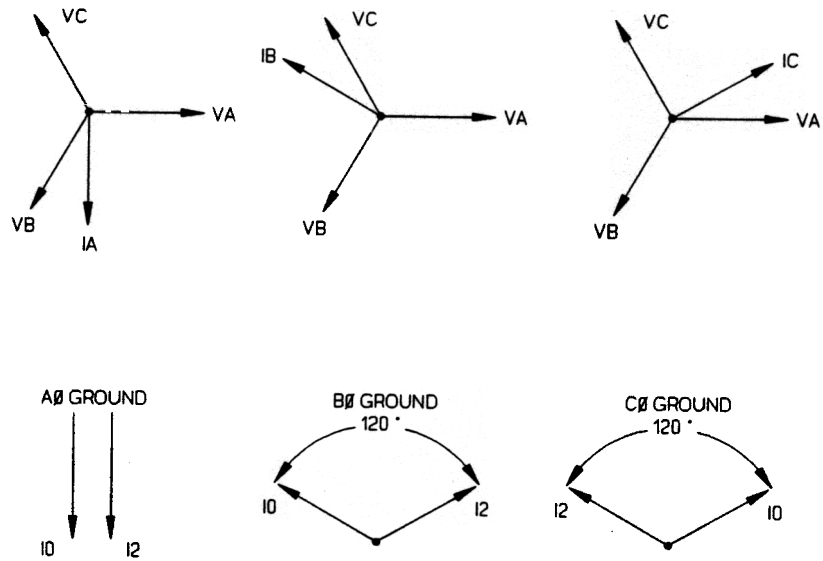


**Figure 15:  $I_0$  and  $I_2$  Relationship for AG, BG, and CG Faults**

Given that the fault is a single-line-ground (SLG) fault, the angle between  $I_0$  and  $I_2$  in the fault is a very reliable indicator of the fault type: centered around zero degrees for AG,  $-120^\circ$  for BG ( $I_2$  lags  $I_0$  by  $120^\circ$ ), and  $+120^\circ$  for CG ( $I_2$  leads  $I_0$  by  $120^\circ$ ). Fortunately, these angles do not change much over a broad range of system conditions.

Thinking about Figures 14 and 15 at the same time, we conclude:

If the angle is near zero, then the fault is AG or BCG.

- If it is AG, then AB or CA could also pick up and three-pole trip for a single-line-ground fault.
- If it is BCG, then the BG and CG ground distance elements may overreach.
- THEREFORE: Enable AG, BC elements only.

If the angle is near  $-120^\circ$ , then the fault is BG or CAG.

- Enable BG and CA elements only.

If the angle is near  $+120^\circ$ , then the fault is CG or ABG.

- Enable CG and AB elements only.
- One approach is to assign  $120^\circ$  sectors to AG, BG and CG faults. For example, angles between  $\pm 60^\circ$  belong to AG and BCG faults.

### **Fault Resistance Can Affect This Scheme**

Figure 16 shows the effects of introducing fault resistance between the point where phases B and C are shorted together and ground.  $R_f$  appears in the zero-sequence network, and the angle of the  $I_0$  leads the angle of  $I_2$ , because the network zero-sequence impedance angle is less than that of the negative-sequence impedance angle.



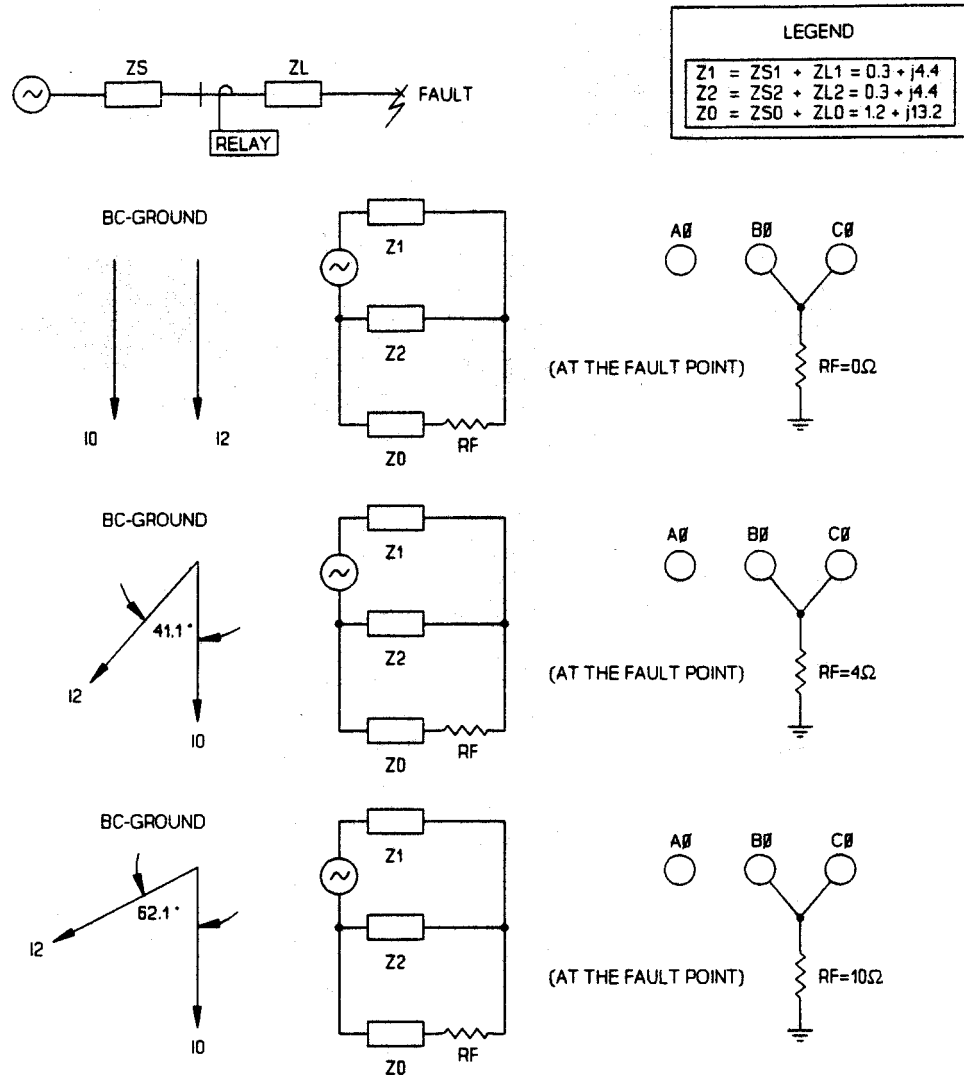


**Figure 16: Effects of Increasing Rf for a BCG Fault**

When Rf is big enough, there may be confusion as to whether the fault is AG/BCG or BG/CAG, because the angle could be less than  $-60^\circ$ , as shown in the bottom of the figure.

**Estimating and Comparing Fault Resistances Solves the Problem**

When the angle itself is not conclusive, e.g., when the angle is more than  $30^\circ$  from its expected value, we can compare phase and ground fault resistance estimates, and select the fault type associated with the minimum resistance. For example, and again referring to the bottom of Figure 16, a comparison of an estimate of Rbg against the minimum phase-to-phase fault resistance (in this case, Rbc), would reveal that Rbg is much larger than Rbc. Therefore, the logic concludes the fault mainly involves phases B and C, and the best measurement is made by the BC element.

## SUMMARY

Important points presented in this paper include:

1. A review of several types of phase-angle comparators shows their similarities and differences.
2. A multiple-input comparator can be viewed as a family of two-input comparators, which includes every pair of inputs.
3. Writing the torque equation for a relay characteristic, setting it equal to zero, and solving for a scalar multiple of the element reach yields a result which maps points on the characteristic onto a single point on the number line. This makes for very efficient synthesis of a family of characteristics with different reaches.
4. Positive-sequence memory potential is generally the most secure and reliable polarization method for mho characteristics.
5. A negative-sequence element which calculates negative-sequence impedance, and tests it against thresholds is presented. It is easy to adapt to virtually any system conditions, because its two threshold settings relate to system impedances.
6. We present ground-fault-resistance elements for quadrilateral characteristics, which estimate the fault resistance, and use the fault-current estimate  $1.5 \cdot (I_0 + I_2)$ . This estimate rejects the load-influenced positive-sequence current, but includes the rest of the fault current.
7. A negative-sequence directional check is sufficient to overcome security problems with phase and ground distance elements for unbalanced faults.
8. A positive-sequence directional element can be used to cut off part of the mho characteristics in the second quadrant of the impedance plane, to enhance security for three-phase faults. This element would normally be set with a maximum torque angle much less than that of the mho circle.
9. Instead of shaping impedance-plane tripping characteristics to avoid load, we introduced a load characteristic. Impedances must leave the load characteristic, before tripping is permitted for three-phase faults. The load characteristic looks like a bow-tie without the knot, and therefore neatly surrounds load areas. It minimizes the area of the impedance plane eliminated for load considerations.
10. We point out a potential problem with fault-type-selectors based on the angle between  $I_0$  and  $I_2$ . They may err for certain resistive LLG faults. The solution is a comparison of estimates of LL and LG fault resistances.

## REFERENCES

- R.J. Martilla, "Directional Characteristics of Distance Relay Mho Elements: Part II - Results." IEEE Transactions on Power Apparatus and Systems, Vol. PAS-100, No.1 January 1981.
2. Edmund O. Schweitzer III, "New Developments in Distance Relay Polarization and Fault Type Selection," 16th Annual Western Protective Relay Conference, October 24 - 26, 1989, Spokane, WA.
  3. A.R. Van C. Warrington, "Protective Relays: Their Theory and Practice." Chapman and Hall, 1969, Volume I and II.

## BIOGRAPHICAL SKETCHES

**Edmund O. Schweitzer** received BSEE and MSEE degrees from Purdue University in 1968 and 1971, respectively. He earned a PhD at Washington State University (WSU) in 1977. His professional experience includes electrical engineering work at Probe Systems in California and the National Security Agency in Maryland. He served as an assistant professor at Ohio University and as an assistant and an associate professor at WSU. Since 1983, he has directed the activities of Schweitzer Engineering Laboratories, Inc. (SEL), the company he founded in Pullman, Washington. SEL designs, manufactures, and markets digital protective relays for power system protection.

Schweitzer started investigating digital relays during PhD studies at WSU in 1976, which produced both his doctoral dissertation and SEL. His university research was supported by Bonneville Power Administration, Electric Power Research Institute, and various utilities. Although the company has grown significantly, Schweitzer is still involved in the development of new relays and auxiliary equipment.

He is a Fellow of the Institute of Electrical and Electronic Engineers (IEEE), is a member of Eta Kappa Nu and Tau Beta Pi, and has authored or co-authored 30 technical papers.

**Jeff B. Roberts** received his BSEE from Washington State University in 1985. He worked for Pacific Gas and Electric Company as a relay protection engineer for over three years. In November, 1988 he joined Schweitzer Engineering Laboratories, Inc. as an Application Engineer. He now serves as Application Engineering Supervisor. He has delivered papers at the Western Protective Relay Conference, Texas A&M University and the Southern African Conference on Power System Protection. He holds one patent on the SEL-121B relay and has other patents pending.

Copyright © SEL 1992, 1993  
(All rights reserved)  
Printed in USA  
Rev. 2